NIH Public Access
Author Manuscript
Cell Microbiol. Author manuscript; available in PMC 2008 July 14.

Published in final edited form as:
Cell Microbiol. 2007 April ; 9(4): 977–987.

Characterization of the interaction between anthrax toxin and its cellular receptors

Shihui Liu[*], **Howard J. Leung**, and **Stephen H. Leppla**
Bacterial Toxins and Therapeutics Section, Laboratory of Bacterial Diseases, National Institute of Allergy and Infectious Diseases, National Institutes of Health, Bethesda, Maryland 20892

Summary

Mutations in capillary morphogenesis gene 2 (*CMG2*), one of the two closely related proteins that act as anthrax toxin receptors, cause two rare human autosomal recessive conditions, juvenile hyaline fibromatosis (JHF) and infantile systemic hyalinosis (ISH). Here we demonstrate that CMG2 proteins with certain JHF- and ISH-associated single amino acid substitutions in their von Willebrand factor A domain or transmembrane region do not function as anthrax toxin receptors. However, an ISH-associated CMG2 variant having a truncated cytosolic domain does still function as an anthrax receptor, and in fact makes cells hyper-sensitive to toxin, distinguishing the roles of CMG2 in physiology and anthrax pathology. Site-specific mutagenesis was used to characterize the role that domain 2 of the anthrax toxin protective antigen (PA) plays in interaction with CMG2, focusing on the interaction between the PA $2\beta_3$–$2\beta_4$ loop and a pocket (Glu-122 pocket) adjacent to the metal ion-dependent adhesion site in CMG2. Substitutions that disrupted the salt bridge between PA Arg-344 and CMG2 Glu-122 decreased the affinity of PA to CMG2 3~4-fold. Furthermore, mutation of CMG2 Tyr-119 (within the Glu-122 pocket) to His lowered the pH threshold for PA prepore-to-pore conversion in the endocytic pathway.

Introduction

Anthrax toxin is a major virulence factor of *Bacillus anthracis*, consisting of three protein subunits: protective antigen (PA, 83 kDa), edema factor (EF, 90 kDa), and lethal factor (LF, 89 kDa) (Liu *et al.*, 2003). These three proteins are individually non-toxic, but can assemble on the cell surface to form a toxic complex. To intoxicate host mammalian cells, PA binds to its cellular receptors (Bradley *et al.*, 2001;Scobie *et al.*, 2003), and is then proteolytically processed to the active form, cell-surface bound PA63. This spontaneously oligomerizes to form PA63 heptamer prepores having EF and LF specific binding sites that bridge two adjacent PA63 subunits, resulting in the final assembly of PA/EF or PA/LF toxin complex on the cell surface (Mourez *et al.*, 2002). Heptamerization of PA63 also triggers the toxin complex internalization by a lipid raft-mediated clathrin-dependent process (Abrami *et al.*, 2003). Recently, the ubiquitously-expressed cell surface protein low density lipoprotein receptor-related protein 6 (LRP6) was found to form a complex with TEM8 and CMG2, and this association is required for internalization of the receptor-toxin complexes into host cells (Wei *et al.*, 2006). In endosomes, the PA63 prepore converts to an LF and EF translocation-competent pore, triggered by an acidic pH environment, and probably involving conformational changes resulting from protonation of several histidine residues in the

* For correspondence: E-mail, shliu@niaid.nih.gov; 301 451 6413 (Tel.); 301 480 0326 (Fax).

Publisher's Disclaimer: This PDF receipt will only be used as the basis for generating PubMed Central (PMC) documents. PMC documents will be made available for review after conversion (approx. 2−3 weeks time). Any corrections that need to be made will be done at that time. No materials will be released to PMC without the approval of an author. Only the PMC documents will appear on PubMed Central -- this PDF Receipt will not appear on PubMed Central.

NIH-PA Author Manuscript
NIH-PA Author Manuscript
NIH-PA Author Manuscript

NIH-PA Author Manuscript

NIH-PA Author Manuscript

NIH-PA Author Manuscript

membrane insertion loop ($2\beta_2-2\beta_3$ loop) of PA domain 2 (Petosa *et al.*, 1997). Therefore, PA is the central part of anthrax toxin, serving as the delivery vehicle for binding and translocation of LF and EF into cytosol of cell to exert their cellular toxic effects (Duesbery *et al.*, 1998;Leppla, 1982;Vitale *et al.*, 2000).

Two homologous cellular membrane proteins, termed tumor endothelium marker 8 (TEM8, also named anthrax toxin receptor 1) and capillary morphogenesis gene 2 product (CMG2, also named anthrax toxin receptor 2), were identified as anthrax toxin receptors (Bradley *et al.*, 2001;Scobie *et al.*, 2003). The exact physiological functions of these two proteins are not known. These proteins contain a signal peptide, a single extracellular von Willebrand factor A (VWA) domain, a single-pass transmembrane region (TM) for plasma membrane anchoring, and a cytosolic tail that might be involved in cytoskeleton interaction and is subject to certain post-translational modifications (Abrami *et al.*, 2006). The VWA domains of CMG2 and TEM8 contain a typical metal ion-dependent adhesion site (MIDAS) motif (DxSxS...T...D, where x can be any amino acid). This site mediates specific binding to collagen IV and laminin (Bell *et al.*, 2001;Dowling *et al.*, 2003;Nanda *et al.*, 2004), indicating that these proteins may function as adhesive molecules mediating cell and extracellular matrix adhesion. TEM8 is reported to be upregulated in colorectal cancer endothelium (St Croix *et al.*, 2000), thus serving as a candidate for tumor targeting. Recently, mutations within *CMG2* have been identified as causing two rare human autosomal recessive conditions, juvenile hyaline fibromatosis (JHF) and infantile systemic hyalinosis (ISH) (Dowling *et al.*, 2003;Hanks *et al.*, 2003). JHF and ISH share many similarities, characterized by multiple subcutaneous skin nodules, gingival hypertrophy, joint contractures, and hyaline deposition (Dowling *et al.*, 2003;Hanks *et al.*, 2003). ISH is the more severe disorder probably due to the greater extent of functional loss of CMG2 in these patients, with onset of the disease at birth or within the first few months of life, often leading to death in infancy due to multisystem failure. Previously, we showed that the cytosolic tail of TEM8 is not essential for the protein to act as a PA receptor (Liu and Leppla, 2003b). While mutations in the extracellular part of CMG2 can cause these diseases, interestingly, alterations in the cytosolic domain also caused ISH, attesting to the physiological importance of the CMG2 cytosolic domain (Dowling *et al.*, 2003;Hanks *et al.*, 2003).

Recently, the crystal structures of the complex of monomeric PA and CMG2 and the complex of heptameric PA63 with seven CMG2 have been solved (Lacy *et al.*, 2004a;Santelli *et al.*, 2004). The results revealed that in addition to the binding of PA domain 4 to the MIDAS region of CMG2, there is an unexpected interaction between a well-ordered loop ($2\beta_3-2\beta_4$) of PA domain 2 and a CMG2 pocket (termed Glu-122 pocket hereafter because the residue Glu-122 is located at the bottom of the pocket) adjacent to the MIDAS motif. By mutational analysis, we show that the salt bridge between PA Arg-344 and CMG2 Glu-122 plays a role in mediating interaction of PA and its receptor. In particular, disturbance of the interaction between the PA $2\beta_3-2\beta_4$ loop and the CMG2 Glu-122 pocket enables PA prepore-to-pore conversion to occur at earlier points in the endocytic pathway. We also found that while the mutations in the VWA domain and TM region of CMG2 that are associated with JHF and ISH impair CMG2 function as anthrax toxin receptors, a physiologically non-functional CMG2 variant having a truncated cytosolic domain does still function as an anthrax receptor. This distinguishes the roles of CMG2 in physiology and pathogenesis.

Results

Functional analyses of receptor mutations mimicking those in JHF and ISH

To investigate whether the physiologically defective CMG2 proteins found in JHF and ISH patients still function as anthrax toxin receptors, we constructed three CMG2 mutants identified in patients (Fig. 1A): CMG2-L45P (with 662T to C mutation in CMG2 cDNA; numbering according to Genbank code AK091721) with Leu-45 changed to Pro at the extracellular VWA

NIH-PA Author Manuscript

NIH-PA Author Manuscript

NIH-PA Author Manuscript

domain (Hanks *et al.*, 2003), CMG2-L329R (1517T to G) with a Leu-329 mutated to Arg in the putative TM region (Dowling *et al.*, 2003;Hanks *et al.*, 2003), and CMG2-P357insC with a nucleotide-C insertion between nucleotides1601−1602 (Dowling *et al.*, 2003;Hanks *et al.*, 2003). In CMG2-P357insC, the one nucleotide-C insertion causes a frameshift mutation, incorporation of a non-native 12–amino acid carboxyl-tail, and a premature downstream stop codon, resulting in the loss of the terminal 132 amino acid residues that constitutes the major part of the cytoplasmic domain (Dowling *et al.*, 2003;Hanks *et al.*, 2003) (Fig. 1A). While the CMG2-L329R mutation causes JFH, those in CMG2-L45P and CMG2-P357insC result in the more severe ISH (Dowling *et al.*, 2003;Hanks *et al.*, 2003), suggesting that CMG2-L329R retains higher residual function than do CMG2-L45P and CMG2-P357insC. Along with these CMG2 mutants, we also constructed the TM and cytosolic domains truncated mutant CMG2-ED (containing residues 1−318) (Fig. 1A).

The various receptor-expressing plasmids were transfected into PR230, a spontaneous PA receptor-deficient CHO cell line described previously (Liu and Leppla, 2003b). Stably transfected, hygromycin-resistant colonies were isolated for each construct. We found that all the colonies transfected with CMG2-L45P (33 clones), CMG2-L329R (32 clones), and CMG2-ED (37 clones) remained resistant to PA + FP59, a recombinant fusion toxin consisting of anthrax toxin LF amino acids 1−254 (LFn) fused to the ADP-ribosylation domain of *Pseudomonas aeruginosa* exotoxin A. In contrast, 50−60% of the colonies transfected with CMG2-P357insC (13 out of 23 clones), like those transfected with wild-type CMG2 (14 out of 28 clones) and TEM8 (15 out of 21 clones), became sensitive to PA plus FP59. RT-PCR analyses indicated that all the transfected CMG2 cDNA constructs were well expressed in the representative clones analyzed, regardless of whether the construct acted as a toxin receptor (Fig. 1D). We showed that the clones transfected with CMG2-P357insC, wild-type CMG2, and human TEM8 could bind and process PA to the active oligomeric form, and were sensitive to PA + FP59 (the results of the representative clones were shown in Fig. 1, B-C). In contrast, the mutants that did not act as toxin receptors, CMG2-L45P, CMG2-L329R, and CMG2-ED, did not support normal levels of toxin binding and oligomer formation. These results showed that the membrane surface location and the extracellular structural integrity of CMG2 are absolutely required for its physiological function as well as for it in acting as an anthrax toxin receptor.

The behavior of the CMG2-P357insC receptor provides additional insights on functional requirements. Expression of this truncated receptor made cells hyper-sensitive to the toxin (Fig. 1B), demonstrating that the intracellular domain of CMG2 is not required for anthrax toxin action. This is consistent with the prior finding that the cytosolic tail of TEM8 is not required for toxin uptake and action (Liu and Leppla, 2003b). Interestingly, the cells transfected with CMG2-P357insC demonstrated stronger binding of PA, thereby providing a plausible explanation for the greater toxin sensitivity of these cells. To determine whether this difference is caused by an increase in PA binding affinity, we measured the apparent affinity (K_d) of PA to the cell surface CMG2 and CMG2-P357insC using competitive Schild Plot analyses (Liu *et al.*, 2005;Malatynska *et al.*, 1998;Varughese *et al.*, 1999). Cytotoxicity assays were performed in the presence of the non-toxic PA protein, PA-U7, in which the furin cleavage sequence RKKR is changed to PGG (Liu *et al.*, 2001). Addition of fixed concentrations of PA-U7 shifted the cytotoxicity dose-response curves rightward (Fig. 2). The EC_{50}s of PA (the concentration needed to kill 50% of the cells) in the presence of various fixed concentrations of PA-U7 were then determined. Prism program was used to perform a non-liner regression to fit the EC_{50}s of PA to the equation Y=-Log(X+10Log K_d)-P (where Y=-Log[EC_{50}] (nM), X=[PA-U7] (nM), P is a constant, see http://www.graphpad.com/curvefit/schild.htm for detailed discussion) to determine K_ds of PA-U7 to the receptor-expressing cells (Fig. 2 and Table 1). The results showed that the apparent affinities of PA-U7 to CMG2-P357insC and wild-type CMG2 are nearly the same (3.5 nM and 3.2 nM, respectively) (Fig. 2 and Table 1). This result,

NIH-PA Author Manuscript

NIH-PA Author Manuscript

NIH-PA Author Manuscript

combined with that of Fig 1*C*, suggests that the PR230-CMG2-P357insC cells possess higher levels of the truncated CMG2 receptor on their cell surface and this explains their greater sensitivity (lower EC_{50}). The higher expression was often observed in other CMG2-P357insC expressing clones. This could occur if one role of the cytosolic tail of CMG2 is to cause constitutive internalization of the receptor, so that the truncated receptor would abnormally accumulate on the surface.

The role of the salt bridge between PA domain 2 (Arg-344) and CMG2 (Glu-122) in anthrax toxin action

Crystal structures of PA bound to CMG2 were determined recently (Lacy *et al.*, 2004a;Santelli *et al.*, 2004). The results revealed that in addition to the binding of PA domain 4 to the MIDAS region of CMG2, there is an unexpected interaction between a well-ordered loop ($2\beta_3-2\beta_4$) of PA domain 2 and a CMG2 pocket (Glu-122 pocket) adjacent to the MIDAS motif. The domain 2 interaction buries approximately 600 $Å^2$ of surface area, compared to the 1,300 $Å^2$ of surface area buried by the domain 4 interaction. The CMG2 pocket is formed by several residues that are conserved in TEM8, including Tyr-119, His-121, Glu-122, and Tyr-158 (refer to Figure 4 in (Santelli *et al.*, 2004) and Figure 2 in (Lacy *et al.*, 2004a)), suggesting their importance in the interaction of PA with CMG2 and TEM8. Tyr-119 and Tyr-158 along with CMG2 β_4-α_4 form the sides of the pocket and His-121 and Glu-122 form its base. These residues are not found in other VWA-containing proteins, such as a 641-residue mouse anthrax toxin receptor-like protein (Genbank accession BAC36683, hereafter referred as ATRL). PA Arg-344 is located at the tip of $2\beta_3-2\beta_4$ and buried within the interface, suggesting it forms a salt bridge with Glu-122 of CMG2. To characterize the role of this additional protein-protein interaction in anthrax toxin action, we mutated PA Arg-344 to the oppositely charged residue Glu to disrupt the electrostatic interaction. We found that PA-R344E could still bind to both CMG2 and TEM8 expressing cells, and mediated cytotoxicity to these cells when used with FP59 (Fig. 3A). However, the toxicity of PA-R344E (when combined with FP59) was approximately 3-fold lower than that of wild-type PA. To directly evaluate the affinity changes, we performed Schild Plot analyses using PA-U7 and PA-R344E-U7 (a non-cleavable PA-R344E with furin site RKKR changed to PGG) as PA competitors. Two previously characterized CMG2-overexpressing cell lines, PR230-CMG2-C4 and TEM8-overexpressing cell line PR230-TEM8-T4, were used because these express approximately similar amounts of PA receptors (Abi-Habib *et al.*, 2005). We found that the apparent affinity of PA-R344E-U7 to CMG2-expressing cells (K_d = 12.5 nM) was approximately 4-fold decreased when compared with that of PA-U7 (K_d = 3.5 nM; Fig. 3B and Table 1). Likewise, the apparent affinity of PA-R344E-U7 (K_d = 83.6 nM) to TEM8-expressing cells was approximately 9-fold decreased (K_d = 9.5 nM for PA-U7) (Fig. 3B and Table 1). These results demonstrated that disruption of the salt bridge between Arg-344 of PA and Glu-122 of CMG2 and the corresponding residue in TEM8 decreases the affinity of PA to CMG2 and TEM8. The role of the salt bridge was further supported by complementing the PA Arg-344 mutation using a charge-reversal mutation in CMG2. Thus, PR230 cells transfected with CMG2-E122K, in which Glu-122 was reversed to the positively charged Lys (Fig. 3C), were more sensitive to the PA-R344E than to wild-type PA. Specifically, we found that PA-R344E displayed 5−6-fold higher toxicity than wild-type PA did to CMG2-E122K expressing cells (Fig. 3C).

To determine whether other conserved residues adjacent to Glu-122 play a role in the PA-CMG2 interaction, we mutated CMG2 Tyr-119 and His-121 to His-119 and Gln-121, so as to match the residues present at the corresponding positions in ATRL (Genbank accession BAC36683), which does not function as a PA receptor (data not shown). Receptors were constructed containing one or both of these amino acid substitutions. The resulting constructs CMG2-Y119H, CMG2-H121Q, and CMG2-Y119H/H121Q were transfected into PR230 cells and analyzed. We found that all three CMG2 mutants could function as PA receptors in

NIH-PA Author Manuscript

NIH-PA Author Manuscript

NIH-PA Author Manuscript

sensitizing the cells to PA plus FP59 (Fig. 4 and data not shown). Furthermore, Schild Plot analyses showed that these mutations did not significantly affect the apparent affinity of PA to cell surface CMG2 (Fig. 4 and Table 1).

In this study, we found that the apparent affinity of PA-U7 (and by implication, wild-type PA) to TEM8-expressing cells was about 3-fold lower than that to CMG2-expressing cells (K_d = 9.5 nM vs. K_d = 3.2~3.5 nM, Fig. 3B and Table 1).

Disturbance of the PA domain 2 interaction with CMG2 lowers the pH threshold for prepore-to-pore conversion

Previous work showed that PA63 heptamer prepores bound to TEM8 do not require as low a pH for conversion to functional pores as do CMG2-bound heptamers (Rainey *et al.*, 2005). The implication is that functional pores may form earlier in the endocytic pathway when heptamers are bound to TEM8 than to CMG2. Experimentally, this difference can be demonstrated by use of ammonium chloride, an agent that neutralizes protons and increases the pH of endosomes. We confirmed that 10 mM ammonium chloride has a strong protective effect on PA + FP59 toxicity to PA230-CMG2 cells, but only a very small protective effect on PR230-TEM8 cells (Fig. 5, A and B). Interestingly, the protective effect was slightly less toward PA-R344E plus FP59 in which the salt bridge between PA Arg-344 and CMG2 Glu-122 was disrupted (Fig. 5B). This subtle but consistent loss in protection could be rescued by restoration of the salt bridge; ammonium chloride conferred full protection to CMG2-E122K expressing cells against PA-R344E plus FP59, but in contrast, less protection to wild-type PA plus FP59 (Fig. 5C). These results suggest that disruption of the salt bridge between PA Arg-344 and CMG2 Glu-122 allows PA prepore-to-pore conversion to occur at an earlier point in the endocytic pathway via weakening the interaction and releasing of PA domain 2 from its receptors. To further evaluate whether changes in other residues in the CMG2 Glu-122 pocket affect the pH-dependent PA prepore-to-pore conversion, we performed the ammonium chloride protection assay on CMG2-Y119H/H121Q cells. We found that PR230-CMG2-Y119H/H121Q cells behaved just like PR230-TEM8 cells, in that ammonium chloride could not confer protection to these cells (Fig. 5F). Further analyses of PR230 cells expressing the individual mutations CMG2-Y119H or CMG2-H121Q alone showed that the loss of ammonium chloride protection phenotype was contributed mainly by Tyr-119 to His mutation rather than His-121 to Gln mutation (Fig. 5, D and E). Although CMG2 Tyr-119 does not contribute to a measurable degree to the interaction between PA and cell surface CMG2 in a neutral environment as shown above (Fig. 4), it appears to play a role in enhancing the binding of the PA Arg-344 $2\beta_3$–$2\beta_4$ loop to the CMG2 Glu-122 pocket within endocytic vesicles, thereby preventing the prepore-to-pore conversion from occurring at near neutral pH.

Discussion

CMG2 and TEM8 are two similar VWA-containing proteins that act as anthrax toxin receptors. The normal physiological roles of these two proteins remain unclear. However, the recent identification of CMG2 mutations as the causes of the two related human conditions JHF and ISH demonstrates the physiological importance and functional nonredundancy of CMG2, even though there exist the highly homologous TEM8 protein (Dowling *et al.*, 2003;Hanks *et al.*, 2003). To study whether the JHF- and ISH- associated CMG2 mutants also lose their function as anthrax toxin receptors, we constructed three CMG2 mutants, CMG2-L45P, CMG2-L329R, and CMG2-P357insC, to mimic those found in JHF and ISH patients. These CMG2 mutants were transfected into the anthrax toxin receptor-deficient PR230 cells. Because highly specific and sensitive CMG2 antibodies are not available, Western blot analyses to evaluate the expression levels of the transfected CMG2 proteins were inconclusive. However, we found that cytotoxicity assays using PA combined with FP59 provided a very sensitive way to

NIH-PA Author Manuscript

NIH-PA Author Manuscript

NIH-PA Author Manuscript

measure the anthrax toxin receptor activity of the transfected CMG2 proteins on cell surface of PR230 cells, which do not express endogenous CMG2 and TEM8. This high sensitivity is due to the enzymatic nature of FP59, so that just a few molecules are required to be translocated into the cytosol of cells to inactivate the translational elongation factor-2, leading to cell death. By analyzing significant numbers of hygromycin-resistant stably transfected clones (about 30 clones for each construct), we found about 50−60% of the clones transfected with wild-type CMG2, CMG2-P357insC, and other functional receptors became sensitive to PA plus FP59, whereas, in contrast, none of the clones transfected with CMG2-L45P and CMG2-L329R did so. RT-PCR analyses revealed that CMG2 constructs did express in the clones tested. Theses results demonstrate that CMG2-L45P and CMG2-L329R, with the ISH- and JHF-associated single amino acid substitutions in their VWA and TM regions, do not function as anthrax toxin receptors. However, CMG2-P357insC, an ISH-associated CMG2 variant having a truncated cytosolic domain does still function as an anthrax receptor, thereby distinguishing the roles of CMG2 in physiology and anthrax pathology.

Leu-45 is a highly conserved core residue located within β1 and hydrophobic pocket II of CMG2 (Lacy *et al.*, 2004b). The unique structural properties of proline and the rarity of this residue within β-strands suggest that mutation in CMG2-L45P would destabilize the molecule in the open high-affinity conformation, thus affecting its function (Lacy *et al.*, 2004b). In CMG2-L329R, the altered CMG2 leucine is in the center of a stretch of five contiguous leucine residues within the putative TM region. This change from hydrophobic to charged amino acid alters the calculated hydropathy and charge profile of the TM domain, possibly resulting in the loss of cell-surface anchoring ability. The data presented here demonstrate that certain mutations in the VWA and TM domains of CMG2 that cause JHF and ISH also appear to eliminate this protein's ability to act as an anthrax toxin receptor, possibly by disrupting the extracellular domain's structure integrity or by preventing normal trafficking to, and retention on, the cell surface. The importance of these extracellular interactions is highlighted by the fact that the defective CMG2-P357insC found in ISH can still act as an anthrax toxin receptor. Although the cytosolic tails of TEM8 and CMG2 are not absolutely required for their function as anthrax toxin receptors, a recent study showed that the efficiency of the receptor function of these proteins can be positively regulated by palmitoylation and ubiquitination of their cytosolic tails (Abrami *et al.*, 2006). Although no physiological role has yet been defined for the cytosolic tail, it would be expected that this truncated cytoplasmic part should be normally an important modulator in signal transduction across the cell membrane. In fact, two Wiskott-Aldrich syndrome protein-homology 1 domains are present in this region (Bell *et al.*, 2001), and, therefore, loss of both of these domains could result in loss of the potential interaction with the actin cytoskeleton.

In this study, we have successfully used Schild Plot non-linear regression analyses to evaluate the apparent affinities of PA proteins for PA receptor-expressing cells. The apparent affinities obtained are readily reproducible with very little variations from experiment to experiment, and are not affected by receptor expression levels, provided the tested cells are sensitive to the toxins in the cytotoxicity assay. We found that the apparent affinity of PA-U7 (and by implication, wild-type PA) to TEM8-expressing cells was 3-fold lower than that to CMG2-expressing cells (K_d = 9.5 nM vs K_d = 3.2~3.5 nM, Fig. 3B). A previous study reported that the disassociation constant of PA to a purified extracellular domain preparation of CMG2 produced as a recombinant protein from CHO cells is as low as 0.17 nM, while that to the extracellular domain of TEM8 produced from *Escherichia coli* is approximately 765-fold higher (130 nM) (Scobie *et al.*, 2005). The method used here to determine affinity constants directly accesses receptors in their native environments, and allows comparison of TEM8 and CMG2 under identical conditions. Although the receptors are normally glycosylated when produced in this way (our unpublished work), this is unlikely to significantly alter their affinity. More important is the fact that expression in mammalian cells avoids any uncertainty about

NIH-PA Author Manuscript

NIH-PA Author Manuscript

NIH-PA Author Manuscript

whether the proteins have folded correctly. Thus, we argue that the apparent disassociation constants reported here are more likely to accurately reflect the behavior of the receptors. The fact that PA binds 3-fold more weakly to TEM8 than to CMG2 may have important consequences to their comparative intracellular trafficking behavior, as discussed below.

We also characterized more fully the role of PA domain 2 in receptor recognition. Although PA binding is mainly determined by the interaction between PA domain 4 and MIDAS motif of CMG2 and TEM8, here we showed that the salt bridge between PA Arg-344 and CMG2 Glu-122 (and the corresponding Glu in TEM8) also contribute to the specific binding of PA and its cellular receptors; disruption of this electrostatic interaction decreases the apparent affinities of PA to CMG2 and TEM8 by about 4- or 9-fold, respectively.

The previous structural study showed that the interaction between PA $2\beta_3{-}2\beta_4$ loop and the CMG2 Glu-122 pocket traps PA membrane insertion loop $2\beta_2{-}2\beta_3$ in a groove between domains 2 and 4 of the neighboring monomer (Lacy *et al.*, 2004a), and this interaction has to be disrupted to free the membrane insertion loop to allow the PA63 heptamer prepore-to-pore conversion to occur (Lacy *et al.*, 2004a;Santelli *et al.*, 2004), a process believed driven by protonation of yet uncharacterized crucial residues located on the interfaces of PA and its receptor. Previous work showed that PA63 heptamer prepores bound to TEM8 do not require as low a pH for conversion to functional pores as do CMG2-bound heptamers (Rainey *et al.*, 2005), indicating that functional pores may form earlier in the endocytic pathway when heptamers are bound to TEM8 than to CMG2. In this study, we demonstrate that disturbance of the interaction between $2\beta_3{-}2\beta_4$ loop of PA and Glu-122 pocket of CMG2, in particular by mutation of CMG2 Tyr-119 to His, lowers the pH threshold for PA prepore-to-pore conversion in the endocytic pathway because ammonium chloride could not confer protection to the mutated CMG2-expressing cells. These CMG2 mutations can be viewed as producing a lower affinity receptor that has properties like those of TEM8. Although CMG2 Tyr-119 does not contribute to a measurable degree to the interaction between PA and cell surface CMG2 in a neutral environment as shown above (Fig. 4), it appears to play a role in enhancing the binding of the PA Arg-344 $2\beta_3{-}2\beta_4$ loop to the CMG2 Glu-122 pocket within endocytic vesicles, thereby preventing the prepore-to-pore conversion from occurring at near neutral pH.

The identifications of TEM8 and CMG2 as anthrax toxin receptors have greatly advanced our knowledge of anthrax toxin in pathogenesis. The results reported here provide further insight into understanding of the interaction of anthrax toxin and the host mammalian cells. Further studies to understand the biological relevance of CMG2 and TEM8 in anthrax pathogenesis would be benefited from the generation of CMG2 and TEM8 null mice.

Experimental procedures

Construction and purification of PA proteins and fusion protein 59

A DNA fragment with the PA Arg-344 to Glu mutation was amplified using 5' primer R344E (primers used in this study are listed in Table 1) and 3' primer PA3, and the PA-expressing plasmid pYS5 (Singh *et al.*, 1989) as a template. The PCR product was then digested with *Bcl*I and *Swa*I, and the resulting 491-bp *Bcl*I-*Swa*I fragment was cloned into the *Bci*I and *Swa*I sites of pYS5, yielding the PA-R344E expressing plasmid pYS5-PA-R344E. The 491-bp R344E fragment was also cloned into the *Bci*I and *Swa*I sites of pYS5-U7 (Liu *et al.*, 2001), yielding the PA-R344E-U7 expressing plasmid pYS5-R344E-U7. PA-U7 is a non-toxic variant of PA with the furin site RKKR replaced by PGG (Liu *et al.*, 2001). The plasmids for protein expression were confirmed by DNA sequencing and then transformed into the non-virulent *Bacillus anthracis* strain BH450. BH450 is a protease and sporulation deficient, virulence plasmid-cured strain previously designated MSLL33 (Pomerantsev *et al.*, 2006). The transformants were grown in FA medium (Rosovitz *et al.*, 2003) with 10 μg/ml kanamycin for

NIH-PA Author Manuscript

NIH-PA Author Manuscript

NIH-PA Author Manuscript

12 h at 37°C. The proteins secreted into the culture supernatants were precipitated on Phenyl-Sepharose Fast Flow resin (30 ml per liter supernatant) in the presence of 2 M ammonium sulfate in rotating bottles. The resin was collected and washed and the proteins were eluted using elution buffer (0.3 M ammonium sulfate, 10 mM Tris-HCl, pH 8.0, 0.5 mM EDTA). The eluted proteins were precipitated by adding 2 M ammonium sulfate. The precipitate was collected by centrifugation, dialyzed in 10 mM Tris-HCl, 1 mM EDTA, pH 8.0, and the PA protein was further purified by chromatography on Q-Sepharose Fast Flow column to one prominent band at the expected molecular mass of 83 kDa.

Fusion protein 59 (FP59) is a recombinant fusion toxin consisting of anthrax toxin LF amino acids 1−254 (LFn) fused to the ADP-ribosylation domain of *Pseudomonas aeruginosa* exotoxin A (Arora and Leppla, 1994). To express FP59 in *B. anthracis* strain BH450, we constructed a FP59-expressing plasmid pYS5-FP59 by replacing the mature PA coding sequence in pYS5 with FP59 coding sequence. The resulting pYS5-FP59 plasmid was transformed into BH450, and FP59 protein was then purified to one prominent band with expected size of 53 kDa from the culture supernatant using similar procedures as for PA proteins as described above.

Construction and transfection of human TEM8 and CMG2 variants into CHO PR230 cells

The plasmid containing full-length human TEM8 cDNA was described previously (Liu and Leppla, 2003b). A human CMG2 cDNA encoding the 489 residue variant (Genbank Accession AAP04016) was isolated by PCR from the Human Liver First-Strand cDNA in the kit of the Human Multiple Tissue cDNA Panel 1 (Cat. No. K1420−1, BD Biosciences, Palo Alto, CA), using 5’ primer CMG2−5a and 3’ primer CMG2−3a. The PCR product was digested with *BsiW*I and *Bcl*I, and cloned into the *Bsr*GI and *Bam*HI sites of pIRESHgy2B, resulting in CMG2 expressing plasmid pIRECMG2. pIRESHgy2B is a bicistronic mammalian expression vector containing an attenuated version of the internal ribosome entry site of the encephalomyocarditis virus, which allows both the gene of interest and the hygromycin B selection marker to be translated from a single mRNA (Liu and Leppla, 2003b). To construct CMG2-L45P, we used 5’primer L45P and 3’ primer CMG2−3b to amplify the mutation-containing fragment, which was then digested with *BssH*II and *Nhe*I. The resulting 288-bp *BssH*II-*Nhe*I fragment was then cloned into the *BssH*II and *Nhe*I sites of pIRECMG2, yielding the CMG2-L45P expressing plasmid pIRECMG2-L45P. To construct CMG2-L229R, we used 5’ primer CMG2−5b and 3’ primer L329R to amplify the mutation-containing fragment, which was then digested with *Afl*II and *BamH*I. The resulting 342-bp *Afl*II-*BamH*I fragment was then cloned into the *Afl*II and *BamH*I sites of pIRECMG2, yielding the CMG2-L329R expressing plasmid pIRECMG2-L329R. To construct CMG2-P357InsC, we used 5’ primer P357InsC and 3’ primer CMG2−3a to amplify the mutation-containing fragment, which was then digested with *BamH*I and *Stu*I. The resulting 235-bp *BamH*I-*Stu*I fragment was then cloned into the *BamH*I and *Stu*I sites of pIRECMG2, yielding the CMG2-P357insC expressing plasmid pIRECMG2-P357InsC. To construct CMG2-ED (TM region and cytosolic tail truncated form), we used 5’ primer CMG2 −5a and 3’ primer ED to amplify the truncated fragment, which was then digested with *Afl*II and *BsiW*I. The resulting 284-bp *Afl*II-*BsiW*I fragment was then cloned into the *Afl*II and *BsiW*I sites of pIRECMG2, yielding TM region and cytosolic tail truncated CMG2 expressing plasmid pIRECMG2-ED. To construct CMG2-E122K, CMG2-Y119H, and CMG2-Y119H/H121Q, we used common 5’ primer CMG2−5c paired with 3’ primers E122K, Y119H, and Y119H/H121Q, respectively, to amplify the corresponding mutation-containing fragments. The resulting PCR products were then digested with *BssH*II and *Nhe*I to isolate 288 bp *BssH*II-*Nhe*I mutagenic fragments, and these were then cloned into the *BssH*II and *Nhe*I sites of pIRECMG2, respectively, yielding the mutated CMG2 proteins expressing plasmids pIRECMG2-E122K, pIRECMG2-Y119H, and pIRECMG2-Y119H/H121Q. The correctness of all receptor-expressing plasmids was confirmed by DNA sequencing. The plasmids were

NIH-PA Author Manuscript

NIH-PA Author Manuscript

NIH-PA Author Manuscript

transfected into the anthrax toxin receptor-deficient mutant CHO PR230 cells (Liu and Leppla, 2003b) using Lipofectamine Plus Reagent (Invitrogen, Carlsbad, CA), and stably transfected cells were selected by growth in hygromycin B (500 μg/ml) for two weeks. Hygromycin-resistant colonies were either isolated individually or directly subjected to toxin challenge. All CHO cells were grown in α-minimal essential medium (AMEM) supplemented with 5% fetal calf serum, 2 mM glutamine, 50 μg/ml gentamycin, and 25 mM 4-(2-hydroxyethyl)-1-piperazineethanesulfonic acid (HEPES). To confirm expression of the transfected genes in the hygromycin-resistant clones, RT-PCR analyses were performed using DNaseI-treated total RNAs as templates. For detection of expression of CMG2 constructs, primers CMG2−5b and CMG2−3c were used to amplify a 277-bp CMG2 fragment. The ubiquitously expressed *dph3*, which is required for diphthamide biosynthesis (Liu *et al.*, 2004;Liu and Leppla, 2003a), was amplified as an internal control using primers Dph3−5 and Dph3−3.

Cytotoxicity assay with MTT

Cells were grown in 96-well plates to approximately 50% confluence. Serial dilutions of PA or mutated PA proteins combined with FP59 (constant at 1.9 nM or 100 ng/ml) were added to the cells to give total volumes of 200 μl/well, and incubated for 48 h. Cell viability was then assayed by adding 50 μl of 2.5 mg/ml MTT (3-[4,5-dimethylthiazol-2-yl]-2,5-diphenyltetrazolium bromide) in AMEM as described previously (Liu and Leppla, 2003b). In Schild Plot analyses, the cells were incubated with various concentrations of PA plus FP59 (constant at 1.9 nM) for 1.5 h in the presence of different fixed concentrations of a non-toxic PA competitor, PA-U7 or PA-R344E-U7. Then the toxins were removed and the cells were cultured 48 h for cell viability analyses. In the ammonium chloride protection experiments, the cells were incubated with toxin for 3 h in the presence of 10 mM NH_4Cl, then the toxins were removed and the cells were cultured in the presence of 10 mM NH_4Cl until 48 h for cell viability analyses.

PA binding analyses

Cells grown to confluence in 24-well plates were incubated with regular medium (AMEM supplemented with 5% fetal calf serum) containing 1 μg/ml of PA for 1 h at 37°C, then washed five times with Hank's Balanced Salt Solution (HBSS) (Biofluids, Rockville, MD) to remove unbound PA. The cells were lysed in 100 μl proteases inhibitors-containing modified RIPA lysis buffer (Liu and Leppla, 2003b) and the cell lysates were subjected to SDS-PAGE. The proteins were then transferred to nitrocellulose membranes, followed by Western blotting to detect cell-associated PA species as described (Liu and Leppla, 2003b). Rabbit anti-PA polyclonal antiserum (#5308) was made in our laboratory by immunization with recombinant PA. Secondary goat anti-rabbit IgG-HRP (sc2054) were purchased from Santa Cruz Biotechnology, Inc. (Santa Cruz, CA).

Acknowledgements

This research was supported by the intramural research program of the National Institute of Allergy and Infectious Diseases, National Institutes of Health. We thank Ralph J. Abi-Habib and Arthur E. Frankel for PR230 CMG2-C4 and PR230-TEM8-T4 cells, Andrei Pomerantsev for providing strain BH450, Rasem Fattah for assistance in protein purification, Hailun Wang and Jiamo Lu for technical assistance.

Abbreviations

CMG2, capillary morphogenesis gene 2 product; EF, edema factor; ISH, infantile systemic hyalinosis; JHF, juvenile hyaline fibromatosis; LF, lethal factor; MIDAS, metal ion-dependent adhesion site; PA, protective antigen; TEM8, tumor endothelium marker 8; TM, transmembrane region; VWA, von Willebrand factor A.

NIH-PA Author Manuscript

NIH-PA Author Manuscript

NIH-PA Author Manuscript

References

Abi-Habib RJ, Urieto JO, Liu S, Leppla SH, Duesbery NS, Frankel AE. BRAF status and mitogen-activated protein/extracellular signal-regulated kinase kinase 1/2 activity indicate sensitivity of melanoma cells to anthrax lethal toxin. Mol Cancer Ther 2005;4:1303–1310. [PubMed: 16170021]

Abrami L, Leppla SH, van der Goot FG. Receptor palmitoylation and ubiquitination regulate anthrax toxin endocytosis. J Cell Biol 2006;172:309–320. [PubMed: 16401723]

Abrami L, Liu S, Cosson P, Leppla SH, van der Goot FG. Anthrax toxin triggers endocytosis of its receptor via a lipid raft-mediated clathrin-dependent process. J Cell Biol 2003;160:321–328. [PubMed: 12551953]

Arora N, Leppla SH. Fusions of anthrax toxin lethal factor with shiga toxin and diphtheria toxin enzymatic domains are toxic to mammalian cells. Infect Immun 1994;62:4955–4961. [PubMed: 7927776]

Bell SE, Mavila A, Salazar R, Bayless KJ, Kanagala S, Maxwell SA, et al. Differential gene expression during capillary morphogenesis in 3D collagen matrices: regulated expression of genes involved in basement membrane matrix assembly, cell cycle progression, cellular differentiation and G-protein signaling. J Cell Sci 2001;114:2755–2773. [PubMed: 11683410]

Bradley KA, Mogridge J, Mourez M, Collier RJ, Young JA. Identification of the cellular receptor for anthrax toxin. Nature 2001;414:225–229. [PubMed: 11700562]

Dowling O, Difeo A, Ramirez MC, Tukel T, Narla G, Bonafe L, et al. Mutations in capillary morphogenesis gene-2 result in the allelic disorders juvenile hyaline fibromatosis and infantile systemic hyalinosis. Am J Hum Genet 2003;73:957–966. [PubMed: 12973667]

Duesbery NS, Webb CP, Leppla SH, Gordon VM, Klimpel KR, Copeland TD, et al. Proteolytic inactivation of MAP-kinase-kinase by anthrax lethal factor. Science 1998;280:734–737. [PubMed: 9563949]

Hanks S, Adams S, Douglas J, Arbour L, Atherton DJ, Balci S, et al. Mutations in the gene encoding capillary morphogenesis protein 2 cause juvenile hyaline fibromatosis and infantile systemic hyalinosis. Am J Hum Genet 2003;73:791–800. [PubMed: 14508707]

Lacy DB, Wigelsworth DJ, Melnyk RA, Harrison SC, Collier RJ. Structure of heptameric protective antigen bound to an anthrax toxin receptor: A role for receptor in pH-dependent pore formation. Proc Natl Acad Sci U S A 2004a;101:13147–13151. [PubMed: 15326297]

Lacy DB, Wigelsworth DJ, Scobie HM, Young JA, Collier RJ. Crystal structure of the von Willebrand factor A domain of human capillary morphogenesis protein 2: An anthrax toxin receptor. Proc Natl Acad Sci U S A 2004b;101:6367–6372. [PubMed: 15079089]

Leppla SH. Anthrax toxin edema factor: a bacterial adenylate cyclase that increases cyclic AMP concentrations of eukaryotic cells. Proc Natl Acad Sci U S A 1982;79:3162–3166. [PubMed: 6285339]

Liu S, Bugge TH, Leppla SH. Targeting of tumor cells by cell surface urokinase plasminogen activator-dependent anthrax toxin. J Biol Chem 2001;276:17976–17984. [PubMed: 11278833]

Liu S, Leppla SH. Retroviral insertional mutagenesis identifies a small protein required for synthesis of diphthamide, the target of bacterial ADP-ribosylating toxins. Mol Cell 2003a;12:603–613. [PubMed: 14527407]

Liu S, Leppla SH. Cell surface tumor endothelium marker 8 cytoplasmic tail-independent anthrax toxin binding, proteolytic processing, oligomer formation, and internalization. J Biol Chem 2003b; 278:5227–5234. [PubMed: 12468536]

Liu S, Milne GT, Kuremsky JG, Fink GR, Leppla SH. Identification of the proteins required for biosynthesis of diphthamide, the target of bacterial ADP-ribosylating toxins on translation elongation factor 2. Mol Cell Biol 2004;24:9487–9497. [PubMed: 15485916]

Liu S, Redeye V, Kuremsky JG, Kuhnen M, Molinolo A, Bugge TH, et al. Intermolecular complementation achieves high-specificity tumor targeting by anthrax toxin. Nat Biotechnol 2005;23:725–730. [PubMed: 15895075]

Liu S, Schubert RL, Bugge TH, Leppla SH. Anthrax toxin: structures, functions and tumour targeting. Expert Opin Biol Ther 2003;3:843–853. [PubMed: 12880383]

NIH-PA Author Manuscript

NIH-PA Author Manuscript

NIH-PA Author Manuscript

Malatynska E, Crites G, Yochum A, Kopp R, Giroux ML, Dilsaver SC. Schild regression analysis of antidepressant and bicuculline antagonist effects at the GABAA receptor. Pharmacology 1998;57:117–123. [PubMed: 9691231]

Mourez M, Lacy DB, Cunningham K, Legmann R, Sellman BR, Mogridge J, et al. 2001: a year of major advances in anthrax toxin research. Trends Microbiol 2002;10:287–293. [PubMed: 12088665]

Nanda A, Carson-Walter EB, Seaman S, Barber TD, Stampfl J, Singh S, et al. TEM8 interacts with the cleaved C5 domain of collagen alpha 3(VI). Cancer Res 2004;64:817–820. [PubMed: 14871805]

Petosa C, Collier RJ, Klimpel KR, Leppla SH, Liddington RC. Crystal structure of the anthrax toxin protective antigen. Nature 1997;385:833–838. [PubMed: 9039918]

Pomerantsev AP, Sitaraman R, Galloway CR, Kivovich V, Leppla SH. Genome engineering in *Bacillus anthracis* using Cre recombinase. Infect Immun 2006;74:682–693. [PubMed: 16369025]

Rainey GJ, Wigelsworth DJ, Ryan PL, Scobie HM, Collier RJ, Young JA. Receptor-specific requirements for anthrax toxin delivery into cells. Proc Natl Acad Sci U S A 2005;102:13278–13283. [PubMed: 16141341]

Rosovitz MJ, Schuck P, Varughese M, Chopra AP, Mehra V, Singh Y, et al. Alanine scanning mutations in domain 4 of anthrax toxin protective antigen reveal residues important for binding to the cellular receptor and to a neutralizing monoclonal antibody. J Biol Chem 2003;278:30936–30944. [PubMed: 12771151]

Santelli E, Bankston LA, Leppla SH, Liddington RC. Crystal structure of a complex between anthrax toxin and its host cell receptor. Nature 2004;430:905–908. [PubMed: 15243628]

Scobie HM, Rainey GJ, Bradley KA, Young JA. Human capillary morphogenesis protein 2 functions as an anthrax toxin receptor. Proc Natl Acad Sci U S A 2003;100:5170–5174. [PubMed: 12700348]

Scobie HM, Thomas D, Marlett JM, Destito G, Wigelsworth DJ, Collier RJ, et al. A soluble receptor decoy protects rats against anthrax lethal toxin challenge. J Infect Dis 2005;192:1047–1051. [PubMed: 16107958]

Singh Y, Chaudhary VK, Leppla SH. A deleted variant of *Bacillus anthracis* protective antigen is non-toxic and blocks anthrax toxin action in vivo. J Biol Chem 1989;264:19103–19107. [PubMed: 2509473]

St Croix B, Rago C, Velculescu V, Traverso G, Romans KE, Montgomery E, et al. Genes expressed in human tumor endothelium. Science 2000;289:1197–1202. [PubMed: 10947988]

Varughese M, Teixeira AV, Liu S, Leppla SH. Identification of a receptor-binding region within domain 4 of the protective antigen component of anthrax toxin. Infect Immun 1999;67:1860–1865. [PubMed: 10085028]

Vitale G, Bernardi L, Napolitani G, Mock M, Montecucco C. Susceptibility of mitogen-activated protein kinase kinase family members to proteolysis by anthrax lethal factor. Biochem J 2000;352(Pt 3):739–745. [PubMed: 11104681]

Wei W, Lu Q, Chaudry GJ, Leppla SH, Cohen SN. The LDL receptor-related protein LRP6 mediates internalization and lethality of anthrax toxin. Cell 2006;124:1141–1154. [PubMed: 16564009]

Supplementary Material

Refer to Web version on PubMed Central for supplementary material.

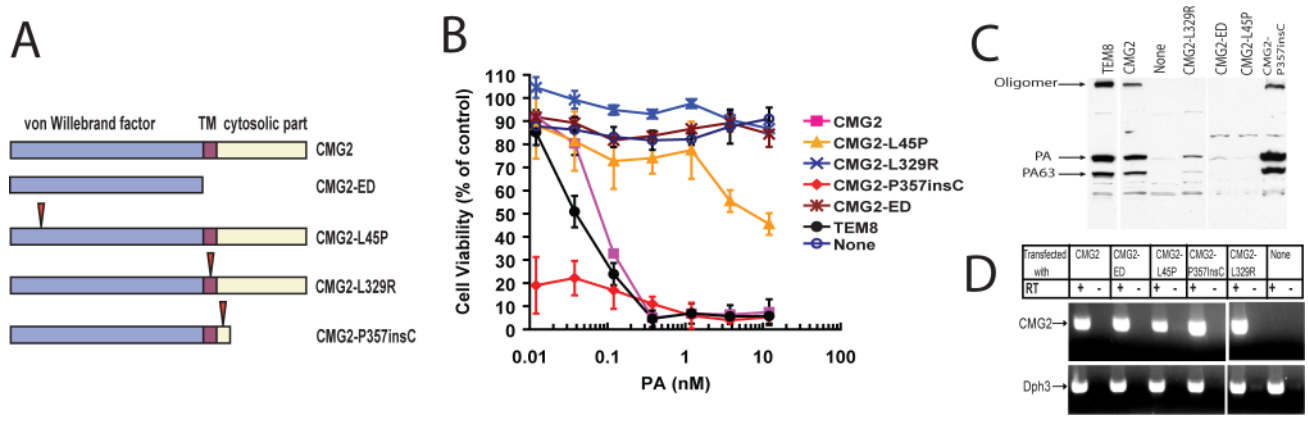

Fig. 1. Functional analyses of CMG2 mutated proteins

A. Schematic representation of the CMG2 constructs. The arrow heads point to the mutation sites. B. Cytotoxicity of PA plus FP59 to representative clones of PR230 cells transfected with various constructs. Cells were incubated with various concentrations of PA plus FP59 (1.9 nM) for 48 h. Cell viability was assessed as described in Experimental procedures. C. Binding of PA to the cells used in panel *B*. The cells were incubated with 1 μg/ml PA at 37 °C for 1 h, washed and lysed. Cell lysates were subjected to SDS-PAGE followed by Western blotting using PA antiserum (#5308). D. RT-PCR analyses of the expression of the transgenes in the clones shown in panels *B* and *C*. The ubiquitously expressed *dph3*, which is required for diphthamide biosynthesis, was amplified as an internal control.

NIH-PA Author Manuscript NIH-PA Author Manuscript NIH-PA Author Manuscript

NIH-PA Author Manuscript

NIH-PA Author Manuscript

NIH-PA Author Manuscript

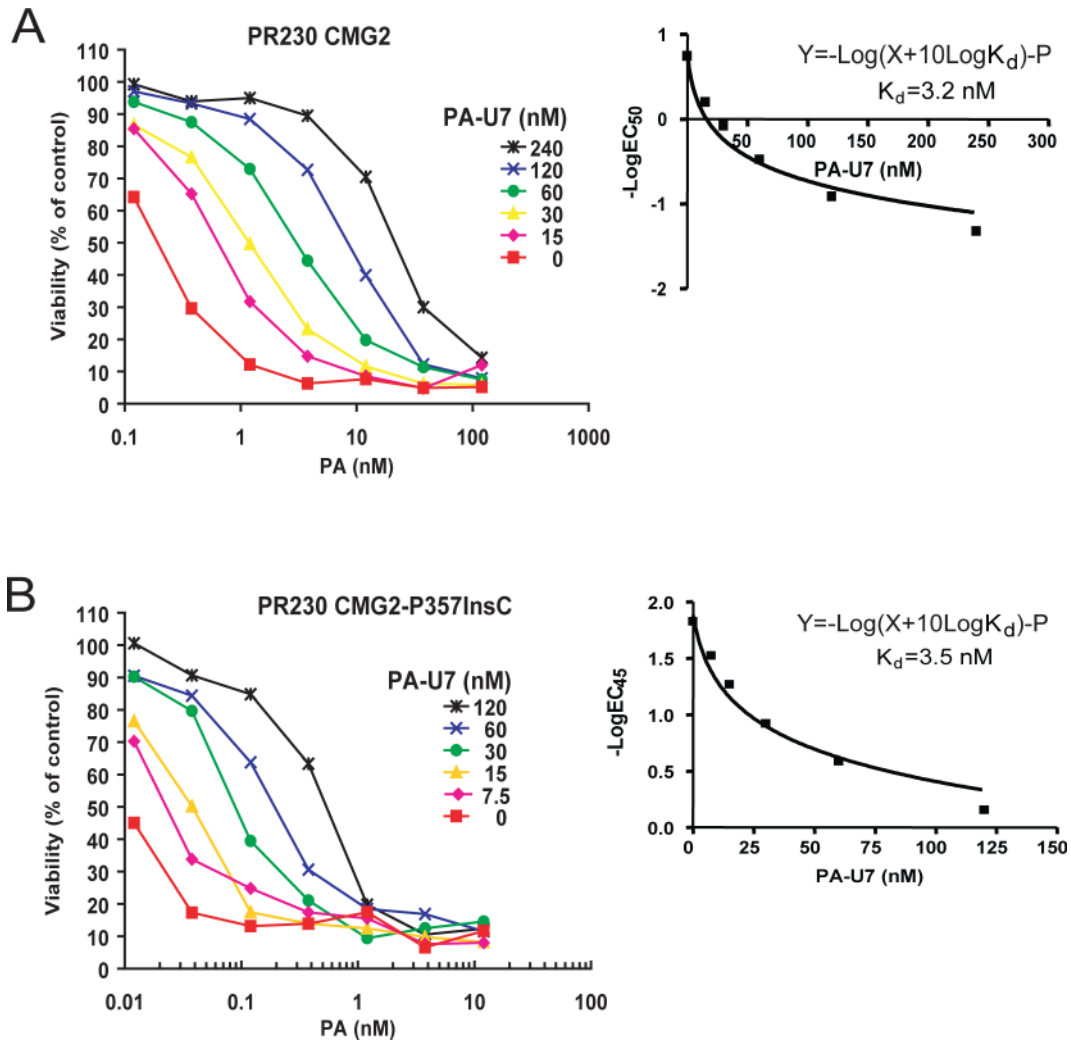

Fig. 2. Evaluation of the apparent binding affinities of PA-U7 to CMG2- and CMG2-P357insC-expressing PR230 cells using Schild Plot analyses

A and B. The CMG2- and CMG2-P357insC-expressing PR230 cells (A and B, respectively) were incubated with various concentrations of PA plus FP59 (1.9 nM) and different concentrations of PA-U7 as indicated for 1.5 h. Then the toxins were removed and the cells were incubated with the toxin-free medium until 48 h when the cell viability was determined. In the Schild Plot analyses, the EC_{50} values (A) or EC_{45} values (B) of PA determined in the presence of various fixed concentrations of PA-U7 were used to fit the equation Y=-Log(X +10Log K_d)-P (where Y=-Log(EC_{50}) (nM), X=[PA-U7] (nM), P is a constant) to determine K_ds of PA-U7 to the receptor-expressing cells. The inserts shown in A and B are the regression curves obtained using Prism program.

NIH-PA Author Manuscript
NIH-PA Author Manuscript
NIH-PA Author Manuscript

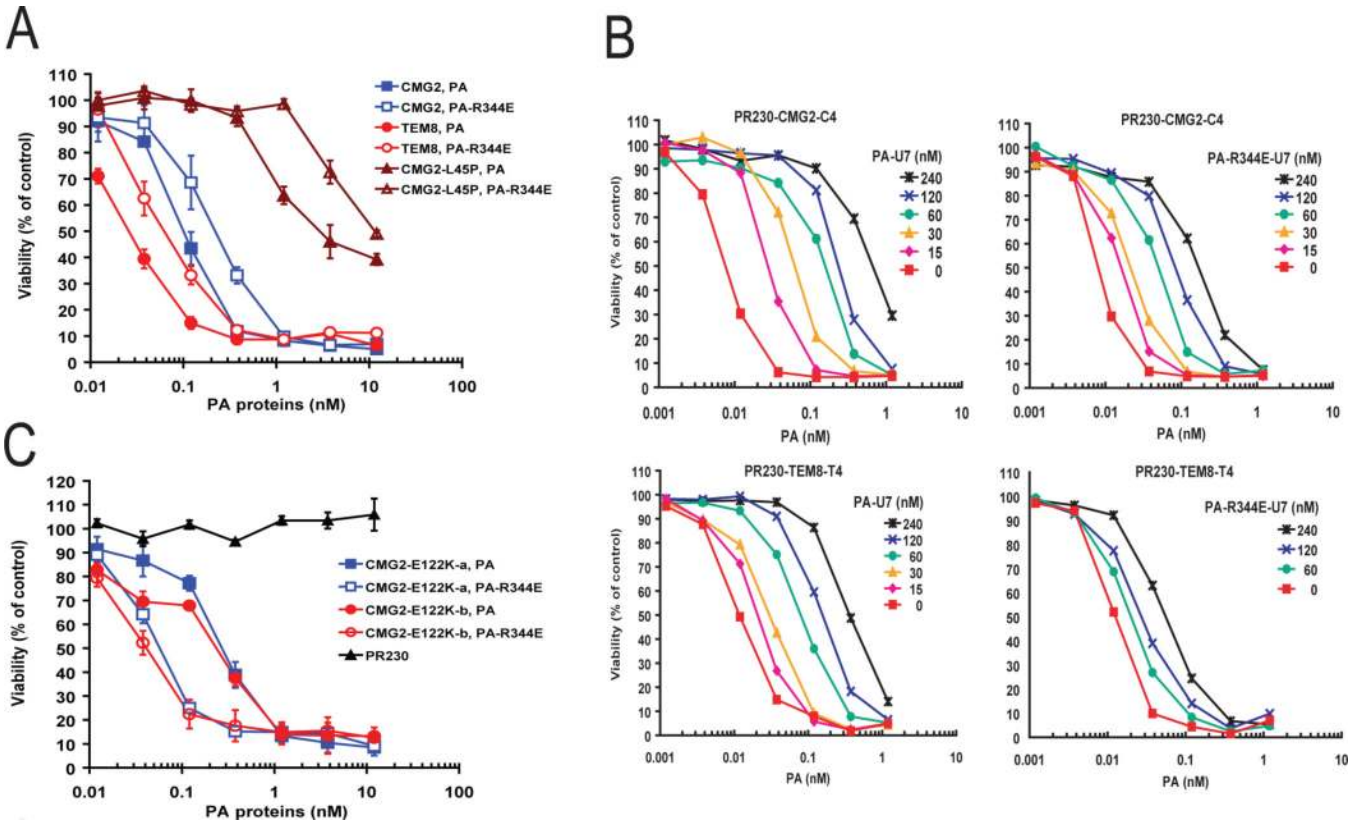

Fig. 3. The salt bridge between PA Arg-344 and CMG2 Glu-122 plays a role in PA and CMG2 interaction

A. Cytotoxicity of PA and PA-R344E (in the presence of FP59) to the TEM8-, CMG2-, and CMG2-L45P expressing PR230 cells. Cells were incubated with various concentrations of PA plus FP59 (1.9 nM) for 48 h, and the cell viability was assessed as in Fig. 1. B. Schild Plot analyses to measure the apparent binding affinities of PA-U7 and PA-R344E-U7 to CMG2- and TEM8-expressing PR230 cells. The analyses were performed as described in Fig. 2. C. PA-R344E is more toxic than PA (in the presence of FP59) to the CMG2-E122K-expressing PR230 cells. Two independent CMG2-E122K-expressing PR230 cell clones (a and b) were incubated with various concentrations of PA or PA-R344E in the presence FP59 (1.9 nM) for 48 h when the cell viability was determined.

NIH-PA Author Manuscript
NIH-PA Author Manuscript
NIH-PA Author Manuscript

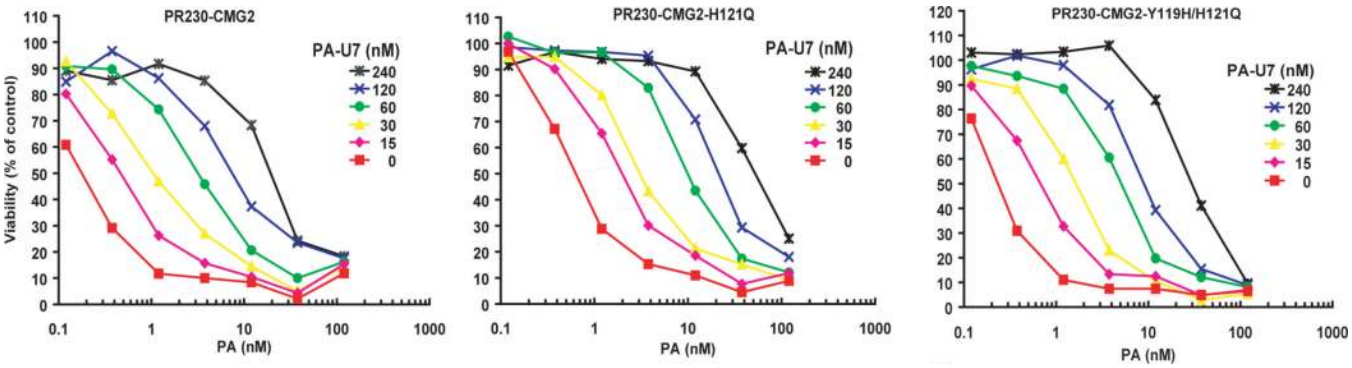

Fig. 4. Certain CMG2 mutations in the CMG2 Glu122 pocket do not affect PA and CMG2 interaction

Schild Plot analyses performed as in Fig. 2 and 3 showed that PA-U7 has similar binging affinity to CMG2-, CMG2-H121Q-, and CMG2-Y119H/H121Q-expressing PR230 cells.

NIH-PA Author Manuscript
NIH-PA Author Manuscript
NIH-PA Author Manuscript

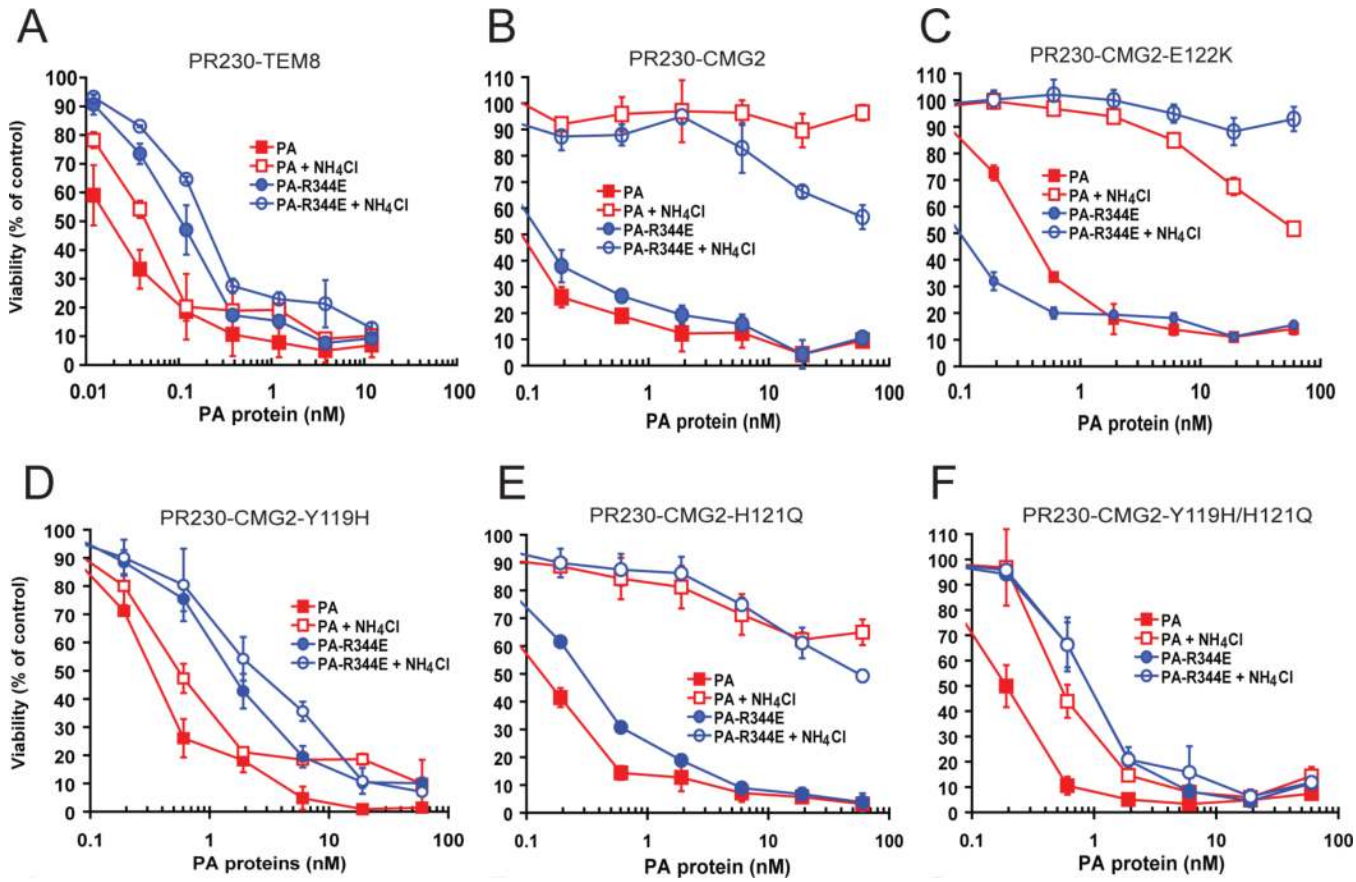

Fig. 5. Disturbance of the interaction between 2β3−2β4 loop of PA and Glu-122 pocket of CMG2 lowers the pH threshold for PA prepore-to-pore conversion

A. Cytotoxicity assays of TEM8-expressing cells challenged with PA or PA-R344E (plus 1.9 nM FP59). The cells were treated with toxins in the absence or presence of 10 mM NH_4Cl for 3 h, then the toxins were removed and the cells were cultured in the presence of 10 mM NH_4Cl for 48 h and cell viability determined. NH_4Cl provided only slight protection. B. Analyses performed as in panel *A* showing that NH_4Cl can fully protect CMG2-expressing PR230 cells from PA plus FP59, but this protection is slightly less effective when the cells were treated with PA-R344E plus FP59, where the salt bridge between PA Arg-344 and CME2 Glu-122 is disrupted. C. Cytotoxicity assays done as above show that CMG2-E122K-expressing cells are more sensitive to PA-R344E than to native PA, due to restoration of the salt bridge, and this strengthened interaction restores high sensitivity to inhibition by NH_4Cl. D-F. Cytotoxicity assays of cells expressing CMG2 having the Tyr119 to His and His121 to Gln substitutions. The Tyr119 to His mutation makes cells largely insensitive to NH_4Cl protection when present alone (Panel D) or in combination with the His121 to Gln substitution (Panel F).

NIH-PA Author Manuscript

NIH-PA Author Manuscript

NIH-PA Author Manuscript

Table 1

Apparent affinities of PA proteins to PA-receptor expressing cells

PA protein	Receptor-expressing cells	K_d (nM)	Source data
PA-U7	PR230-CMG2 (EC_{50}=0.18 nM [a])	3.2[b]	Fig. 2
PA-U7	PR230-CMG2-P357insC	3.5	Fig. 2
PA-U7	PR230-CMG2-C4 (EC_{50}=0.0074 nM [a])	3.5[b]	Fig. 3B
PA-R344E-U7	PR230-CMG2-C4	12.5	Fig. 3B
PA-U7	PR230-TEM8-T4	9.5	Fig. 3B
PA-R344E-U7	PR230-TEM8-T4	83.6	Fig. 3B
PA-U7	PR230-CMG2 (EC_{50}=0.16 nM [a])	3.1[b]	Fig. 4
PA-U7	PR230-CMG2-H121Q	4.0	Fig. 4
PA-U7	PR230-CMG2-Y119H/H121Q	3.1	Fig. 4
PA-U7	PR230-CMG2-Y119H	3.2	Not shown

[a] The EC_{50}s obtained in the corresponding Figures were the PA concentrations needed to kill 50% of the receptor-expressing cells in the absence of PA-U7.

[b] Comparison of these K_ds indicating that the apparent affinities obtained using Schild Plot analysis are not affected by the expression levels of the receptors, and suffer very limited variation from experiment to experiment.